UC Irvine
UC Irvine Previously Published Works

Title
Inhibiting oral intoxication of botulinum neurotoxin A complex by carbohydrate receptor mimics

Permalink
https://escholarship.org/uc/item/6758v8q7

Journal
Toxicon, 107(Pt A)

ISSN
0041-0101

Authors
Lee, Kwangkook
Lam, Kwok-Ho
Kruel, Anna-Magdalena
et al.

Publication Date
2015-12-01

DOI
10.1016/j.toxicon.2015.08.003

Peer reviewed

eScholarship.org Powered by the California Digital Library
University of California

Author Manuscript

Author Manuscript

Author Manuscript

Author Manuscript

HHS Public Access

Author manuscript

Toxicon. Author manuscript; available in PMC 2016 December 01.

Published in final edited form as:

Toxicon. 2015 December 1; 107(0 0): 43–49. doi:10.1016/j.toxicon.2015.08.003.

Inhibiting oral intoxication of botulinum neurotoxin A complex by carbohydrate receptor mimics

Kwangkook Lee[1,†], **Kwok-Ho Lam**[1,†], **Anna-Magdalena Kruel**[2], **Stefan Mahrhold**[2], **Kay Perry**[3], **Luisa W. Cheng**[4], **Andreas Rummel**[2,*], and **Rongsheng Jin**[1,*]

[1]Department of Physiology and Biophysics, University of California, Irvine, CA 92697, USA

[2]Institut für Toxikologie, Medizinische Hochschule Hannover, Hannover, Germany

[3]NE-CAT and Department of Chemistry and Chemical Biology, Cornell University, Building 436E, Argonne National Laboratory, 9700 S. Cass Avenue, Argonne, IL 60439, USA

[4]Foodborne Toxin Detection and Prevention Research Unit, Western Regional Research Center, United States Department of Agriculture, Agricultural Research Service, Albany, CA 94710, USA

Abstract

Botulinum neurotoxins (BoNTs) cause the disease botulism manifested by flaccid paralysis that could be fatal to humans and animals. Oral ingestion of the toxin with contaminated food is one of the most common routes for botulism. BoNT assembles with several auxiliary proteins to survive in the gastrointestinal tract and is subsequently transported through the intestinal epithelium into the general circulation. Several hemagglutinin proteins form a multi-protein complex (HA complex) that recognizes host glycans on the intestinal epithelial cell surface to facilitate BoNT absorption. Blocking carbohydrate binding to the HA complex could significantly inhibit the oral toxicity of BoNT. Here, we identify lactulose, a galactose-containing non-digestible sugar commonly used to treat constipation, as a prototype inhibitor against oral BoNT/A intoxication. As revealed by a crystal structure, lactulose binds to the HA complex at the same site where the host galactose-containing carbohydrate receptors bind. *In vitro* assays using intestinal Caco-2 cells demonstrated that lactulose inhibits HA from compromising the integrity of the epithelial cell monolayers and blocks the internalization of HA. Furthermore, co-administration of lactulose significantly protected mice against BoNT/A oral intoxication *in vivo*. Taken together, these data encourage the development of carbohydrate receptor mimics as a therapeutic intervention to prevent BoNT oral intoxication.

[*]Corresponding authors: rummel.andreas@mh-hannover.de (AR); r.jin@uci.edu (RJ).
[†]Authors contributed equally to this work.

Publisher's Disclaimer: This is a PDF file of an unedited manuscript that has been accepted for publication. As a service to our customers we are providing this early version of the manuscript. The manuscript will undergo copyediting, typesetting, and review of the resulting proof before it is published in its final citable form. Please note that during the production process errors may be discovered which could affect the content, and all legal disclaimers that apply to the journal pertain.

The atomic coordinates and structure factors of the HA17-HA33-lactulose and HA17-HA33-IPTG complexes have been deposited in the Protein Data Bank under the accession codes 5BQU and 5BP5, respectively.

Author Manuscript Author Manuscript Author Manuscript Author Manuscript

Keywords

Botulinum neurotoxin; Hemagglutinin; Progenitor toxin complex; Lactulose; carbohydrate receptor; inhibitor

Introduction

Botulinum neurotoxins (BoNTs) produced by *Clostridium botulinum* are the most poisonous toxins, and classified by the Centers for Disease Control and Prevention as one of the six highest-risk threat agents for bioterrorism (Arnon et al., 2001). They specifically cleave the soluble *N*-ethylmaleimide sensitive factor attachment protein receptors (SNAREs) after invading motoneurons at neuromuscular junctions and subsequently block acetylcholine release (Rossetto et al., 2014). Current treatment for botulism requires early diagnosis, immediate treatment with equine antitoxin, prolonged hospitalization in an intensive care unit and mechanical ventilation (Rusnak and Smith, 2009). Hence, there is an urgent need to develop effective diagnostic and preventive countermeasures against oral BoNT intoxication.

There are seven serotypes of BoNT (termed BoNT/A-G) including at least 40 different subtypes, among which BoNT/A, B, E, and F are known to cause human botulism (Rossetto et al., 2014). BoNTs are naturally secreted in the form of progenitor toxin complex (PTC) where the toxin is bound to several non-toxic neurotoxin-associated proteins (NAPs). NAPs are encoded together with the toxin gene in one of two different gene clusters, the *HA* cluster or the *orfX* cluster (Hill and Smith, 2013). Besides a common non-toxic non-hemagglutinin (NTNHA) protein, the *HA* gene cluster (BoNT/A1–D and G) encodes three hemagglutinins (HA70, HA17, and HA33) and the *orfX* cluster (BoNT/A2–4, E, F) encodes three proteins termed orfX1–3 (Gu and Jin, 2013; Kubota et al., 1998; Lam and Jin, 2015). The function of the orfX proteins remains mysterious, so they will not be included in the following discussion. NAPs are crucial for the delivery of BoNTs across the epithelial barrier into systemic circulation, as BoNTs themselves are sensitive to inactivation and degradation in the hostile environment of the gastrointestinal (GI) tract (Gu et al., 2012; Shone et al., 1985). The oral toxicity of BoNTs is increased by hundreds to thousands folds in the form of PTC compared to the naked toxin (Ohishi, 1984; Ohishi et al., 1977).

The large PTC (L-PTC) contains two structurally and functionally distinct modules. BoNT and NTNHA form an oval-shaped interlocked complex (M-PTC), which protects the toxin against digestive enzymes and the acidic environment in the gut (Gu et al., 2012). The three HAs form an extended three-blade architecture (HA complex) that is composed of HA70, HA17 and HA33 in 3:3:6 stoichiometry (Amatsu et al., 2013; Benefield et al., 2013; Lee et al., 2013). HA70 and HA33 carry an N-acetylneuraminic acid (Neu5Ac) and a galactose (Gal) binding site, respectively. Therefore, each HA complex comprises a total of nine glycan-binding sites, which allow multivalent interactions with host carbohydrates to enrich the toxin complex on the intestinal surface (Lee et al., 2013; Matsumura et al., 2015; Sugawara et al., 2014; Yao et al., 2014). The HA complex then interacts with E-cadherin, a major host adhesion protein, to disrupt the E-cadherin mediated cell-cell adhesion and open

Author Manuscript Author Manuscript Author Manuscript Author Manuscript

the paracellular route facilitating the transepithelial delivery of BoNT (Lee et al., 2014b; Matsumura et al., 2008; Sugawara et al., 2010). Interestingly, a recent study suggests that the carbohydrate-binding activity of HA may help the PTC to exploit microfold (M) cells to breach the intestinal epithelial barrier, which is mediated by glycoprotein 2 (GP2) on the cell surface (Matsumura et al., 2015).

The substantial recent advances in understanding the structure and function of HA-carbohydrate interactions suggest a new strategy for the development of preventive countermeasures for BoNTs based on carbohydrate receptor mimicry. For instance, isopropyl β-D-1-thiogalactopyranoside (IPTG), a non-metabolizable Gal analog, could inhibit the oral toxicity of L-PTC/A using a mouse model (Lee et al., 2013). In this study, we have identified lactulose (LAU), 4-O-β-*D*-galactopyranosyl-D-fructose, as another potential inhibitor. We have performed thermodynamic analysis on binding between HA33 and LAU, and resolved the crystal structure of their complex. The physiological relevance of the HA33-LAU interaction was further examined by an *in vitro* model using Caco-2 epithelial cells and by an *in vivo* mouse oral toxicity assay.

Material and Methods

Construct design and cloning

The constructs of HA70, HA17, and HA33 were prepared as previously reported (Lee et al., 2013). Briefly, full length HA17 (residues M1–I146) and full length HA33 (residues M1–P293) from *C. botulinum* BoNT/A1 were cloned separately into the bicistronic pRSFDuet-1 vector for co-expression. HA17 was produced with an N-terminal 6xHis tag to facilitate protein purification while HA33 carries no tag. Full length HA70 (residues M1-N626) was cloned into the expression vector pQE30.

Protein expression and purification

Protein expression and purification were performed as described previously (Lee et al., 2013). Briefly, HA17 and HA33 were co-expressed in *Escherichia coli* strain BL21-RIL (DE3) (Novagen). The HA17-HA33 complex was first purified by Ni-NTA (nitrilotriacetic acid, Qiagen) affinity column. His-tag was removed by PreScission protease and the protein was further purified by MonoS ion-exchange chromatography and Superdex 200 size-exclusion chromatography. The protein complex was concentrated to ~6 mg/ml using Amicon Ultra centrifugal filter (Millipore) for crystallization. The complete HA complex was reconstituted by mixing HA70 and the HA17-HA33 complex at a molar ratio of ~1:3.9 and the complex was further purified by Superdex 200 chromatography. The fluorescence-labeled HA complex (HA*) was prepared with Alexa Fluor® 488 labeled HA70 and unlabeled HA17- HA33 complex (Lee et al., 2013).

Isothermal titration calorimetry

The calorimetry titration experiments were performed on an ITC200 calorimeter from Microcal/GE Life Sciences (Northampton, MA). LAU (40 mM) was used as the titrant in the syringe and HA33 (200 μM) was used as the titrand in the cell. The data were analyzed

Author Manuscript Author Manuscript Author Manuscript Author Manuscript

using the Origin software package. The thermodynamic values reported are the mean of three independent experiments.

Crystallization, Data collection and Structure Determination

Crystals of the HA17-HA33 complex were prepared as described previously (Lee et al., 2013). Protein-carbohydrate complexes were obtained by soaking the HA17-HA33 crystals with 100 mM IPTG or LAU at 18 °C overnight. X-ray diffraction data were collected at the Advanced Photon Source (APS). The crystals belong to space group $C222_1$, with unit cell dimensions a =107 Å, b = 119 Å, c = 162 Å; $\alpha = \beta = \gamma = 90°$. The data were processed with HKL2000 (Otwinowski and Minor, 1997). Data collection statistics are summarized in Table 1. The structures were determined by molecular replacement software Phaser using apo- HA17-HA33 (PDB code 4LO0) as the search model (Lee et al., 2013; McCoy et al., 2007). Manual model building and refinements were performed using COOT, PHENIX, and CCP4 packages in an iterative manner (Adams et al., 2010; Emsley et al., 2010; Winn et al., 2011). IPTG and LAU were modeled into the corresponding structure during the refinement based on the Fo-Fc electron density maps. The refinement progress was monitored with the free R value using a 5% randomly selected test set. The structures showed excellent stereochemistry based on MolProbity validation (Chen et al., 2010). Structural refinement statistics are listed in Table 1. All structure figures were prepared with PyMol. (http://www.pymol.org)

Transwell assay

The transwell assay was performed as previously described (Lee et al., 2013; Lee et al., 2014b). Caco-2 cells were obtained from the German Cancer Research Center (Heidelberg, Germany). The cells were subcultured twice a week and seeded on BD Falcon Cell Culture Inserts (0.9 cm^2) at a density of approximately 10^5 cells cm^{-2} for flux studies and determination of transepithelial electrical resistance (TER). All TER experiments were conducted in 0.5 ml and 1.5 ml of Iscoves Modified Dulbeccos Medium without phenol red in the apical and basolateral reservoir, respectively. LAU (95%, Sigma-Aldrich, Taufkirchen, Germany) was dissolved in IMDM, sterile filtered and stored at −20°C. The HA* were pre-incubated with LAU overnight at 4°C in IMDM and diluted to the final concentration with IMDM prior to administration. The TER upon administration of LAU in the highest concentrations used was checked in the absence of HA* and was virtually identical to that of the control without sugars. The HA* was administered to the apical or basolateral reservoirs at final concentrations of 58 nM and 17 nM, respectively. TER was determined with an epithelial volt-ohm meter (World Precision Instruments, Berlin, Germany) equipped with an Endohm 12 chamber for filter inserts. Only filters with an initial resistance of ≥300 Ω cm^{-2} were used. For analysis of independent experiments subsequent results were expressed as percentages of the corresponding resistance of each data set determined immediately after administration of samples. Values are expressed as means of ≥3 independent experiments with duplicate samples ± standard deviations. For paracellular transport studies, 200 μl of samples were taken from the apical and the basolateral reservoir after 24 hour of incubation. The fluorescence signal was measured in a BioTek Synergy 4 fluorescence spectrophotometer at 495 nm excitation and 519 nm emission wavelengths.

Author Manuscript Author Manuscript Author Manuscript Author Manuscript

Inhibition of oral intoxication

Oral mouse intoxication was performed as previously described (Cheng et al., 2008). Sets of 15–30 female Swiss Webster mice (4–5 weeks old, 20–23 g) were used per test sample. Mice were treated by gavage via a popper needle with 100 μl containing 3.0 μg of L-PTC/A (Metabiologics) in phosphate gelatin buffer (10 mM phosphate buffer pH 6.2 and 2% gelatin), with or without 250 or 500 mM of LAU and IPTG, respectively. Mice were monitored for botulism symptoms for up to 14 days post-intoxication. Median survival and p-values were determined with the GraphPad Prism 6 program (San Diego, CA). Animal studies were performed according to approved animal use protocols by the Animal Use and Care Committee of the USDA.

Influence of LAU and IPTG on neurotoxicity

The influence of IPTG and LAU on the neurotoxicity of isolated, recombinant wild-type BoNT/A was determined using the mouse phrenic nerve (MPN) hemidiaphragm assay. The free BoNT/A (1.6 pM) was pre-incubated for 15 min at 37°C in 4 ml Kreb-Ringer media without or with 50 mM IPTG and LAU, respectively, and then applied to the organ bath containing the hemidiaphragm tissue. The MPN hemidiaphragm assay was performed as described previously (Rummel et al., 2004). The phrenic nerve was continuously stimulated at 5–25 mA with a frequency of 1 Hz and a pulse duration of 0.1 ms. Isometric contractions were transformed using a force transducer and recorded with VitroDat Online software (FMI GmbH, Seeheim, Germany). The time required to decrease the amplitude to 50% of the starting value (paralytic half-time) was determined.

Results

Lactulose binds to the HA complex

A comprehensive glycan array study suggested that HA33 has a strong preference for carbohydrates bearing a terminal Gal (Yao et al., 2014). It has been shown that Gal and lactose (Lac) could protect Caco-2 cell monolayers from being damaged by the HA complex, likely by competing with the endogenous carbohydrate receptors on the cell surface. However, they were not able to protect mice in an oral intoxication model (Lee et al., 2013). In contrast, the non-metabolizable Gal analog IPTG could significantly extend the median survival time of mice (Lee et al., 2013). These findings suggest that non-digestible Gal-containing carbohydrates could be more desirable to function in the gut. In an effort to further explore the potential carbohydrate receptor mimics, we have identified LAU as a promising candidate. LAU is a synthetic disaccharide that is non-digestible in the small intestine but can be degraded by colon bacterial fluora into e.g. lactate. LAU is safe for human consumption (oral LD50 in rat: 18.2 g/kg) and is commonly used as an osmotic laxative to treat chronic constipation and commonly used as food additive (Wesselius-De Casparis et al., 1968). Based on a thermodynamic analysis using isothermal titration calorimetry, we found that LAU bound to HA33 with a dissociation constant (K_d) of ~1.4 mM with 1:1 stoichiometry (Figure 1). The binding affinity is comparable to that of Gal (1.8 mM), N-acetyllactosamine (LacNAc) (1.0 mM), Lac (1.0 mM), and IPTG (0.8 mM) as reported previously (Lee et al., 2013).

Author Manuscript Author Manuscript Author Manuscript Author Manuscript

Structures of LAU- and IPTG-bound HA17-HA33 complex reveal a conserved glycan-binding mode

The HA complex is composed of a trimeric HA70 in the center, with each HA70 docking with one HA17 that further binds to two molecules of HA33 (Figure 2A). HA33 is composed of two β-trefoil domains linked by a short α-helix, and the Gal-binding site is located at the tip of the C-terminal β-trefoil domain (Figure 2B) (Arndt et al., 2005; Lee et al., 2013; Lee et al., 2014a). To gain further insight into the molecular details of how HA33 recognizes Gal analogs, we determined the crystal structures of HA17-HA33 in complex with LAU or IPTG at 2.4 Å and 2.2 Å resolution, respectively. There is one copy of the complex composed of HA17 and HA33 in a 1:2 ratio in one asymmetric unit. The structures of the two HA33 molecules (Chains A and B) are identical. Chain A that displays slightly better electron densities is used in the following discussion.

The crystal structures reveal that LAU and IPTG bind to HA33 in a manner almost identical to that of Gal (Figure 2E–G) (Lee et al., 2013). Six HA33 residues make direct contacts with the Gal moiety of LAU and IPTG, which include hydrogen bonding between Gal with residues Gln276, Asp263, His281, Asn285, and Gly266. In addition, a crucial stacking interaction is formed between Phe278 and the hydrophobic side of the Gal hexose ring. On the other hand, the fructose moiety of LAU and the isopropyl group of IPTG do not directly bind to HA33, and have relatively weak electron densities (Figure 2C–D). This is consistent with our glycan array study, which suggests that HA33 does not have strong preference for additional saccharides other than the terminal Gal (Yao et al., 2014). A water molecule is observed in the IPTG complex that connects Asp283 and Asn285 of HA33 to O4 of IPTG. A similar water molecule was observed in the structures of HA33 bound to Lac or LacNAc, but not in HA33-LAU and HA33-Gal complexes (Figure 2E–G) (Lee et al., 2013).

Lactulose inhibits transport of the HA complex across Caco-2 cell monolayers

The intestinal epithelial cell line Caco-2 has been widely used to characterize the transport of BoNTs *in vitro* (Couesnon et al., 2008; Lee et al., 2013; Matsumura et al., 2008; Sugawara et al., 2014). In a trans-well assay, Caco-2 cells are differentiated on a permeable poly-carbonate support to form a polarized columnar cell monolayer resembling the small intestinal epithelial layer with high transepithelial resistance against passive diffusion of ion and solutes. The HA complex of BoNT/A and BoNT/B could disrupt the integrity of the Caco-2 monolayer, leading to a marked reduction of transepithelial electrical resistance (TER) (Lee et al., 2013; Matsumura et al., 2008). We have previously shown that some carbohydrate receptor mimics could inhibit the HA-mediated reduction of TER by competing with the endogenous carbohydrate receptors for HA binding (Lee et al., 2013). Here, we found that pre-incubation of the HA complex with 15 mM of LAU significantly inhibited the reduction of TER by 67% and 22% when it was applied to the apical or basolateral side of the monolayer, respectively. The inhibitory effect from the basolateral compartment was more profound when 50 mM LAU was applied (Figure 3A–B). Therefore LAU strongly inhibits the HA complex from disrupting Caco-2 monolayers with a higher potency upon apical addition illustrating the importance of the terminal Gal for initial absorption. To further verify this finding, we investigated the effect of LAU on the transport of the fluorescence-labeled HA complex (HA*) across the Caco-2 monolayer (Figure 3C).

Author Manuscript Author Manuscript Author Manuscript Author Manuscript

We found that as low as 5 mM LAU efficiently inhibited the transport of HA* from the apical to the basolateral side and vice versa. Taken together with the previous studies on IPTG and Lac, we conclude that Gal-containing carbohydrates could efficiently inhibit the transport of BoNT/A complex across the intestinal wall *in vitro*.

Lactulose could inhibit BoNT/A oral intoxication

We used a mouse lethality model to further compare the inhibition efficacy of LAU and IPTG on BoNT/A oral toxicity *in vivo* (Lee et al., 2013). IPTG or LAU at 250 mM or 500 mM was co-administrated with L-PTC/A by oral gavage, and the mouse survival time was closely monitored (Figure 4). The median survival time (MST) of the control group was ~37 hrs (dead/live, 24/5, n=29). Remarkably, over half of the intoxicated mice survived the challenge after 14 days with the treatment of LAU at 250 mM (dead/live, 8/12, n=20) or 500 mM (dead/live, 12/18, n=30), or IPTG at 500 mM (dead/live, 3/12, n=15). In comparison, 250 mM IPTG showed no significant protection (dead/live, 11/4, n=15). Therefore the non-digestible LAU displays a higher potency for protection of mice than IPTG.

As an important control, the neurotoxicity of recombinant BoNT/A was determined in the presence of IPTG and LAU, respectively, employing the mouse phrenic nerve hemidiaphragm assay. 50 mM of IPTG or LAU alone did not cause any sign of paralysis of the hemidiaphragm during the acquisition period of >100 min. 1.6 pM of BoNTA caused 50% paralysis within 67.0 ± 4.2 min. Pre-incubation of 1.6 pM BoNT/A with 50 mM IPTG or 50 mM LAU resulted in paralytic half-times of 68.4 ± 10.7 min (SD, n = 5) and 69.2 ± 4.1 min (SD, n = 5), respectively. Hence, IPTG and LAU likely do not bind to the ganglioside-binding site on the toxin and do not directly influence the neurotoxicity of BoNT/A itself.

Discussion

There is an urgent need to develop safe and effective countermeasures against BoNTs. The development of carbohydrate receptor mimics as BoNT inhibitors is attractive because of their low cost and high stability. They are easy to administer, stockpile and transport, and likely cause limited adverse effects. These inhibitors could confer immediate temporary protection in case of intentional release of BoNT or BoNT-producing bacteria. A proof-of-principle study showed that administrating IPTG 1 hour before the BoNT/A oral intoxication was able to extend the survival of intoxicated mice (Lee et al., 2013). In this study, we have identified LAU as another oral inhibitor for further development. LAU may offer an additional advantage since it induces diarrhea while constipation is a typical symptom for botulism patients. This will accelerate clearance of non-absorbed L-PTC from the gut as well as of its producer *C. botulinum* in case of infant botulism.

The multiple glycan-binding sites on the HA complex provide a “Velcro effect” that greatly enhance the binding avidity to glycan on the intestinal surface (Zopf and Roth, 1996). This may be a major reason why simple carbohydrates like IPTG and LAU only showed weak inhibition towards oral BoNT/A intoxication on mice. Therefore, it would be more desirable to develop multivalent carbohydrate inhibitors that simultaneously target multiple receptor-binding sites on the HA complex (Barthelson et al., 1998; Bernardi et al., 2013; Thomas,

Author Manuscript Author Manuscript Author Manuscript Author Manuscript

2010). In fact, decavalent ligands against cholera toxin lead to a 106-fold increase in potency compared with monovalent Gal (Zhang et al., 2002). Although these carbohydrate receptor mimicking inhibitors do prevent but may not cure botulism, they could be used as a secondary treatment for the clearance of toxins remaining in the intestine, or to prevent further intoxication in the cases of intestinal colonization with bacterial spores in intestinal botulism.

Supplementary Material

Refer to Web version on PubMed Central for supplementary material.

Acknowledgments

This work was partly supported by National Institute of Allergy and Infectious Diseases (NIAID) grant R01AI091823 to R.J. and by the Swiss Federal Office for Civil Protection BABS #353003325 to A.R.; L.W.C. was funded by the United States Department of Agriculture, Agricultural Research Service, National Program project NP108, CRIS 5325- 42000-048-00D. NE-CAT at the Advanced Photon Source (APS) is supported by a grant from the National Institute of General Medical Sciences (P41 GM103403). Use of the APS, an Office of Science User Facility operated for the U.S. Department of Energy (DOE) Office of Science by Argonne National Laboratory, was supported by the U.S. DOE under Contract No. DE-AC02-06CH11357.

Abbreviations

BoNT	Botulinum neurotoxin
LAU	Lactulose
HA	Hemagglutinin
PTC	Progenitor toxin complex
NTNHA	Non-toxic non-hemagglutinin

References

Adams PD, Afonine PV, Bunkoczi G, Chen VB, Davis IW, Echols N, Headd JJ, Hung LW, Kapral GJ, Grosse-Kunstleve RW, McCoy AJ, Moriarty NW, Oeffner R, Read RJ, Richardson DC, Richardson JS, Terwilliger TC, Zwart PH. PHENIX: a comprehensive Python-based system for macromolecular structure solution. Acta Crystallogr D Biol Crystallogr. 2010; 66:213–221. [PubMed: 20124702]

Amatsu S, Sugawara Y, Matsumura T, Kitadokoro K, Fujinaga Y. Crystal structure of Clostridium botulinum whole hemagglutinin reveals a huge triskelion-shaped molecular complex. J Biol Chem. 2013; 288:35617–35625. [PubMed: 24165130]

Arndt JW, Gu J, Jaroszewski L, Schwarzenbacher R, Hanson MA, Lebeda FJ, Stevens RC. The structure of the neurotoxin-associated protein HA33/A from Clostridium botulinum suggests a reoccurring beta-trefoil fold in the progenitor toxin complex. J Mol Biol. 2005; 346:1083–1093. [PubMed: 15701519]

Arnon SS, Schechter R, Inglesby TV, Henderson DA, Bartlett JG, Ascher MS, Eitzen E, Fine AD, Hauer J, Layton M, Lillibridge S, Osterholm MT, O'Toole T, Parker G, Perl TM, Russell PK, Swerdlow DL, Tonat K. Botulinum toxin as a biological weapon: medical and public health management. JAMA. 2001; 285:1059–1070. [PubMed: 11209178]

Barthelson R, Mobasseri A, Zopf D, Simon P. Adherence of Streptococcus pneumoniae to respiratory epithelial cells is inhibited by sialylated oligosaccharides. Infect Immun. 1998; 66:1439–1444. [PubMed: 9529065]

Benefield DA, Dessain SK, Shine N, Ohi MD, Lacy DB. Molecular assembly of botulinum neurotoxin progenitor complexes. Proc Natl Acad Sci U S A. 2013; 110:5630–5635. [PubMed: 23509303]

Author Manuscript Author Manuscript Author Manuscript Author Manuscript

Bernardi A, Jimenez-Barbero J, Casnati A, De Castro C, Darbre T, Fieschi F, Finne J, Funken H, Jaeger KE, Lahmann M, Lindhorst TK, Marradi M, Messner P, Molinaro A, Murphy PV, Nativi C, Oscarson S, Penades S, Peri F, Pieters RJ, Renaudet O, Reymond JL, Richichi B, Rojo J, Sansone F, Schaffer C, Turnbull WB, Velasco-Torrijos T, Vidal S, Vincent S, Wennekes T, Zuilhof H, Imberty A. Multivalent glycoconjugates as anti-pathogenic agents. Chem Soc Rev. 2013; 42:4709–4727. [PubMed: 23254759]

Chen VB, Arendall WB 3rd, Headd JJ, Keedy DA, Immormino RM, Kapral GJ, Murray LW, Richardson JS, Richardson DC. MolProbity: all-atom structure validation for macromolecular crystallography. Acta Crystallogr D Biol Crystallogr. 2010; 66:12–21. [PubMed: 20057044]

Cheng LW, Onisko B, Johnson EA, Reader JR, Griffey SM, Larson AE, Tepp WH, Stanker LH, Brandon DL, Carter JM. Effects of purification on the bioavailability of botulinum neurotoxin type A. Toxicology. 2008; 249:123–129. [PubMed: 18538461]

Couesnon A, Pereira Y, Popoff MR. Receptor-mediated transcytosis of botulinum neurotoxin A through intestinal cell monolayers. Cell Microbiol. 2008; 10:375–387. [PubMed: 17900298]

Emsley P, Lohkamp B, Scott WG, Cowtan K. Features and development of Coot. Acta Crystallogr D Biol Crystallogr. 2010; 66:486–501. [PubMed: 20383002]

Gu S, Jin R. Assembly and function of the botulinum neurotoxin progenitor complex. Curr Top Microbiol Immunol. 2013; 364:21–44. [PubMed: 23239347]

Gu S, Rumpel S, Zhou J, Strotmeier J, Bigalke H, Perry K, Shoemaker CB, Rummel A, Jin R. Botulinum neurotoxin is shielded by NTNHA in an interlocked complex. Science. 2012; 335:977–981. [PubMed: 22363010]

Hill KK, Smith TJ. Genetic Diversity Within Clostridium botulinum Serotypes, Botulinum Neurotoxin Gene Clusters and Toxin Subtypes. Curr Top Microbiol Immunol. 2013; 364:1–20. [PubMed: 23239346]

Kubota T, Yonekura N, Hariya Y, Isogai E, Isogai H, Amano K, Fujii N. Gene arrangement in the upstream region of Clostridium botulinum type E and Clostridium butyricum BL6340 progenitor toxin genes is different from that of other types. FEMS Microbiol Lett. 1998; 158:215–221. [PubMed: 9465394]

Lam KH, Jin R. Architecture of the botulinum neurotoxin complex: a molecular machine for protection and delivery. Current opinion in structural biology. 2015; 31:89–95. [PubMed: 25889616]

Lee K, Gu S, Jin L, Le TT, Cheng LW, Strotmeier J, Kruel AM, Yao G, Perry K, Rummel A, Jin R. Structure of a bimodular botulinum neurotoxin complex provides insights into its oral toxicity. PLoS Pathog. 2013; 9:e1003690. [PubMed: 24130488]

Lee K, Lam KH, Kruel AM, Perry K, Rummel A, Jin R. High-resolution crystal structure of HA33 of botulinum neurotoxin type B progenitor toxin complex. Biochem Biophys Res Commun. 2014a; 446:568–573. [PubMed: 24631690]

Lee K, Zhong X, Gu S, Kruel AM, Dorner MB, Perry K, Rummel A, Dong M, Jin R. Molecular basis for disruption of E-cadherin adhesion by botulinum neurotoxin A complex. Science. 2014b; 344:1405–1410. [PubMed: 24948737]

Matsumura T, Jin Y, Kabumoto Y, Takegahara Y, Oguma K, Lencer WI, Fujinaga Y. The HA proteins of botulinum toxin disrupt intestinal epithelial intercellular junctions to increase toxin absorption. Cell Microbiol. 2008; 10:355–364. [PubMed: 17868282]

Matsumura T, Sugawara Y, Yutani M, Amatsu S, Yagita H, Kohda T, Fukuoka S, Nakamura Y, Fukuda S, Hase K, Ohno H, Fujinaga Y. Botulinum toxin A complex exploits intestinal M cells to enter the host and exert neurotoxicity. Nature communications. 2015; 6:6255.

McCoy AJ, Grosse-Kunstleve RW, Adams PD, Winn MD, Storoni LC, Read RJ. Phaser crystallographic software. J Appl Cryst. 2007; 40:658–674. [PubMed: 19461840]

Ohishi I. Oral toxicities of Clostridium botulinum type A and B toxins from different strains. Infect Immun. 1984; 43:487–490. [PubMed: 6693168]

Ohishi I, Sugii S, Sakaguchi G. Oral toxicities of Clostridium botulinum toxins in response to molecular size. Infect Immun. 1977; 16:107–109. [PubMed: 326664]

Otwinowski Z, Minor W. Processing of X-ray diffraction data collected in oscillation mode. Methods Enzymol. 1997; 276:307–326.

Author Manuscript Author Manuscript Author Manuscript Author Manuscript

Rossetto O, Pirazzini M, Montecucco C. Botulinum neurotoxins: genetic, structural and mechanistic insights. Nat Rev Microbiol. 2014; 12:535–549. [PubMed: 24975322]

Rummel A, Mahrhold S, Bigalke H, Binz T. The HCC-domain of botulinum neurotoxins A and B exhibits a singular ganglioside binding site displaying serotype specific carbohydrate interaction. Mol Microbiol. 2004; 51:631–643. [PubMed: 14731268]

Rusnak JM, Smith LA. Botulinum neurotoxin vaccines: Past history and recent developments. Human vaccines. 2009; 5:794–805. [PubMed: 19684478]

Shone CC, Hambleton P, Melling J. Inactivation of Clostridium botulinum type A neurotoxin by trypsin and purification of two tryptic fragments. Proteolytic action near the COOH-terminus of the heavy subunit destroys toxin-binding activity. Eur J Biochem. 1985; 151:75–82. [PubMed: 3896784]

Sugawara Y, Matsumura T, Takegahara Y, Jin Y, Tsukasaki Y, Takeichi M, Fujinaga Y. Botulinum hemagglutinin disrupts the intercellular epithelial barrier by directly binding E-cadherin. J Cell Biol. 2010; 189:691–700. [PubMed: 20457762]

Sugawara Y, Yutani M, Amatsu S, Matsumura T, Fujinaga Y. Functional Dissection of the Clostridium botulinum Type B Hemagglutinin Complex: Identification of the Carbohydrate and E-Cadherin Binding Sites. PLoS One. 2014; 9:e111170. [PubMed: 25340348]

Thomas RJ. Receptor mimicry as novel therapeutic treatment for biothreat agents. Bioengineered bugs. 2010; 1:17–30. [PubMed: 21327124]

Wesselius-De Casparis A, Braadbaart S, Bergh-Bohlken GE, Mimica M. Treatment of chronic constipation with lactulose syrup: results of a double-blind study. Gut. 1968; 9:84–86. [PubMed: 4867936]

Winn MD, Ballard CC, Cowtan KD, Dodson EJ, Emsley P, Evans PR, Keegan RM, Krissinel EB, Leslie AG, McCoy A, McNicholas SJ, Murshudov GN, Pannu NS, Potterton EA, Powell HR, Read RJ, Vagin A, Wilson KS. Overview of the CCP4 suite and current developments. Acta Crystallogr D Biol Crystallogr. 2011; 67:235–242. [PubMed: 21460441]

Yao G, Lee K, Gu S, Lam KH, Jin R. Botulinum Neurotoxin A Complex Recognizes Host Carbohydrates through Its Hemagglutinin Component. Toxins. 2014; 6:624–635. [PubMed: 24525478]

Zhang Z, Merritt EA, Ahn M, Roach C, Hou Z, Verlinde CL, Hol WG, Fan E. Solution and crystallographic studies of branched multivalent ligands that inhibit the receptor-binding of cholera toxin. J Am Chem Soc. 2002; 124:12991–12998. [PubMed: 12405825]

Zopf D, Roth S. Oligosaccharide anti-infective agents. Lancet. 1996; 347:1017–1021. [PubMed: 8606566]

Author Manuscript Author Manuscript Author Manuscript Author Manuscript

Highlights

- Crystal structures of the HA17-HA33 complex bound to lactulose or IPTG were resolved at 2.4 Å and 2.2 Å, respectively.
- Lactulose competes with host carbohydrate receptors for HA binding.
- Lactulose interferes with the transport of the HA complex across Caco-2 cell monolayer *in vitro*.
- Lactulose has a higher potency than IPTG against BoNT/A oral intoxication in mice.

Author Manuscript Author Manuscript Author Manuscript Author Manuscript

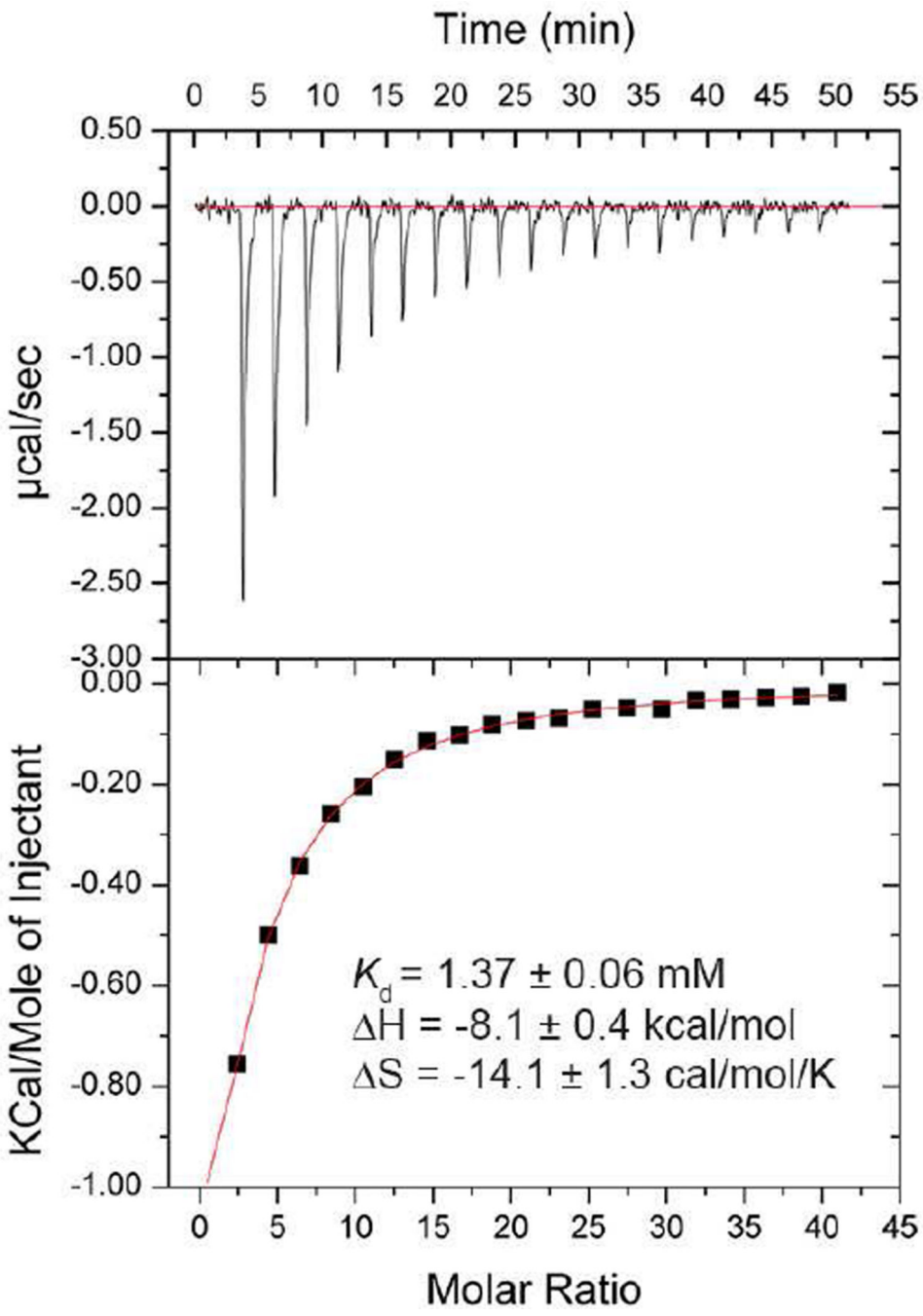

Figure 1. Isothermal titration calorimetry characterization of LAU-HA33 interaction

The experiment was triplicated and a representative titration curve is shown. The thermodynamics parameters are reported as mean ± standard deviation.

Author Manuscript Author Manuscript Author Manuscript Author Manuscript

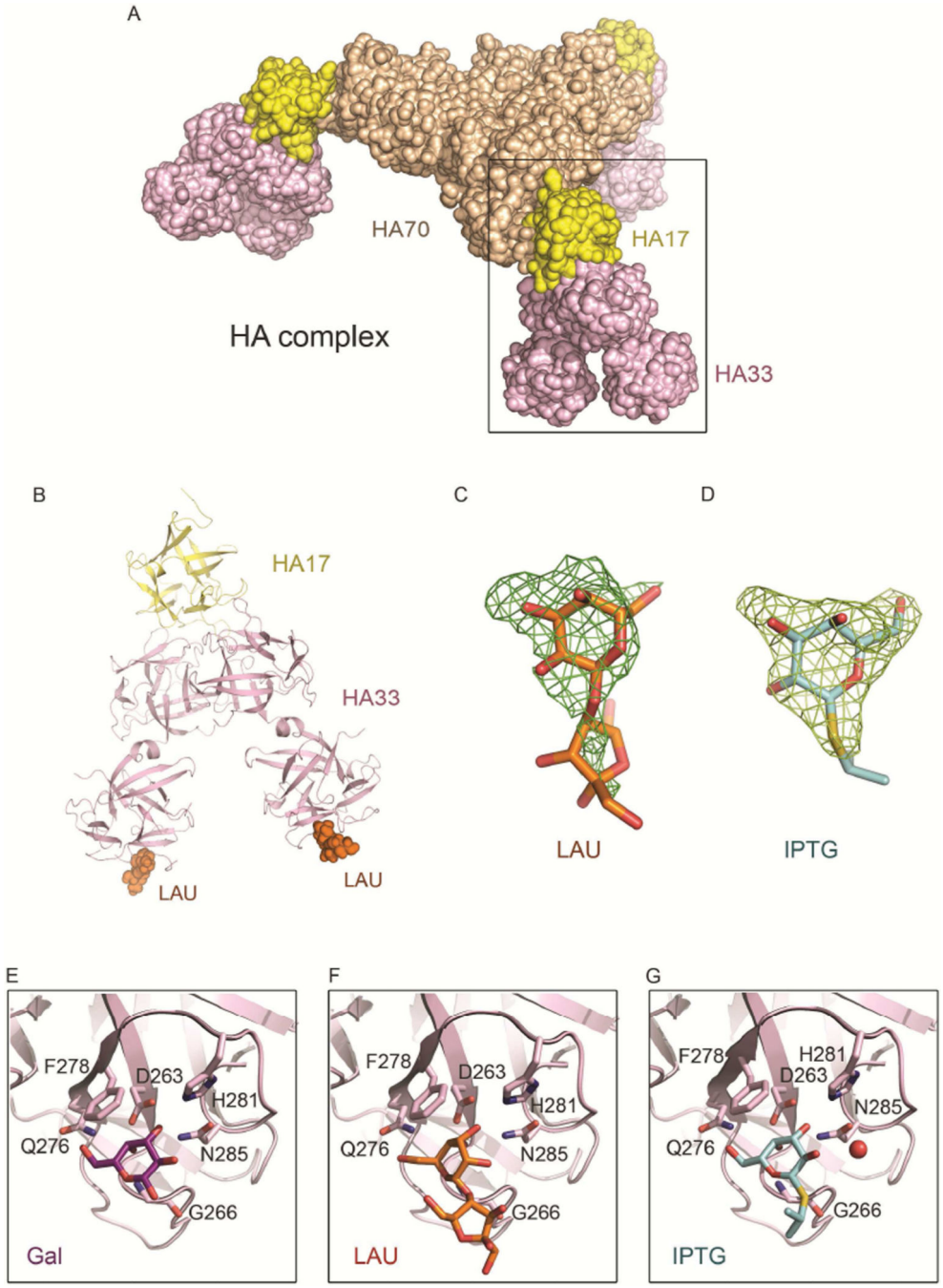

Figure 2. Crystal structures of the HA17-HA33-LAU and HA17-HA33-IPTG complexes indicate a conserved glycan-binding mode

(A) The structure of the HA complex. HA70, HA17, and HA33 are colored wheat, yellow, and pink, respectively. (B) The structure of the HA17-HA33-LAU complex where LAU is drawn as orange spheres. (C–D) The Fo-Fc omit maps (contoured at 3.0 σ) around the bound LAU (orange stick) and IPTG (cyan stick); the ligands were omitted from map calculation. (E–G) Close-up views of the glycan-binding site on HA33. Key residues that mediate the HA33 interaction with Gal (purple), LAU (orange), or IPTG (cyan) are shown as sticks. A

water molecule found in the IPTG complex is drawn as a red sphere. The HA17-HA33-Gal complex is included here for comparison (PDB code: 4LO1) (Lee et al., 2013).

Author Manuscript Author Manuscript Author Manuscript Author Manuscript

Author Manuscript Author Manuscript Author Manuscript Author Manuscript

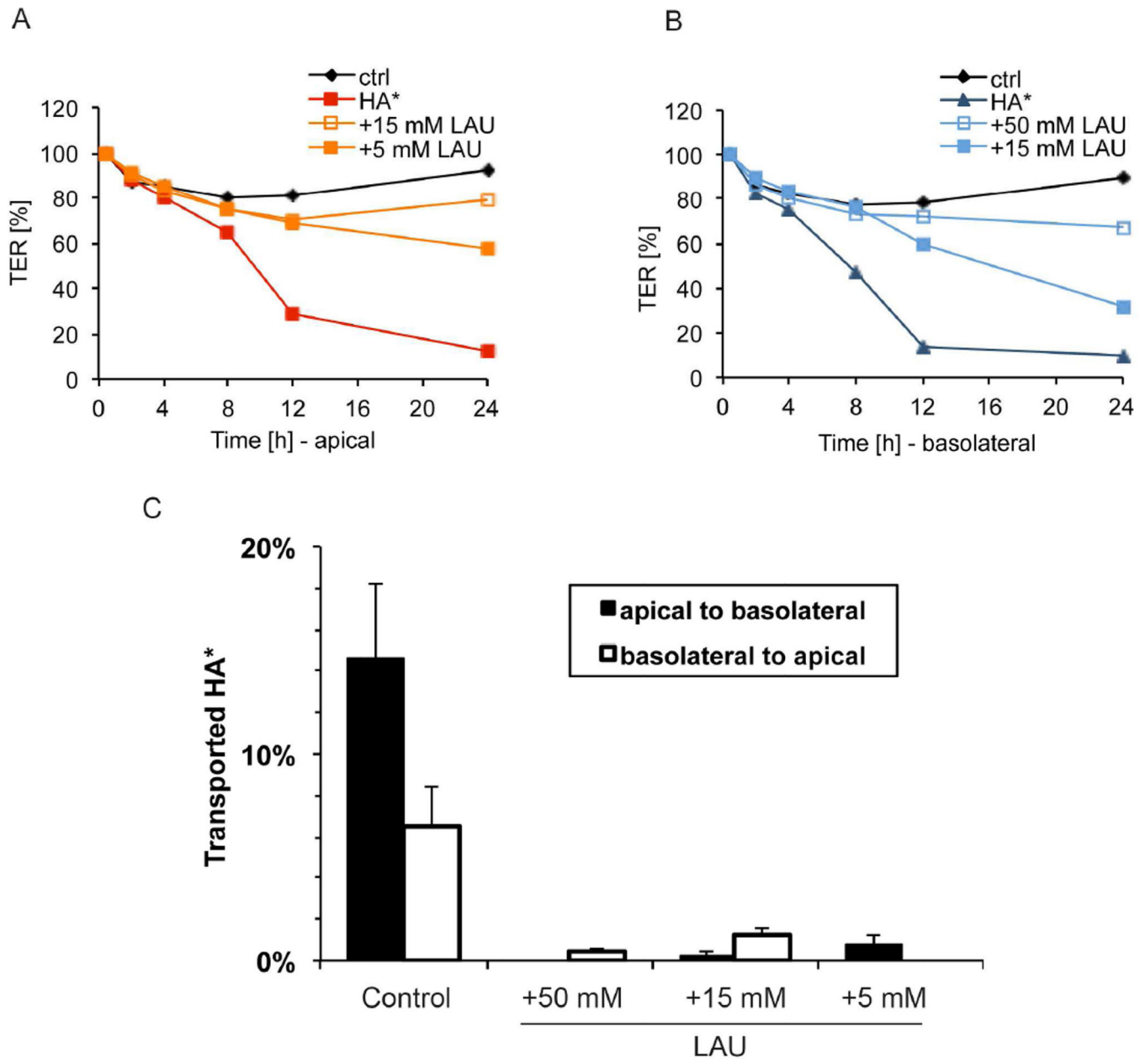

Figure 3. LAU inhibits the HA-mediated reduction of TER of human intestinal Caco-2 cell monolayers

Caco-2 cells were grown on transwell filter membranes into confluent polarized monolayer. (A–B) TER of Caco-2 monolayers was measured when Alexa-488-labeled HA complex (HA*) pre-incubated with LAU was applied to the apical (A; 58 nM of HA*) or basolateral (B; 17 nM of HA*) chamber. Values are means ± SD (n = 4–12). (C) HA* with various concentrations of LAU was applied to the apical (at 58 nM) or basolateral (at 17 nM) chamber. The fluorescence signals in both chambers were quantified after 24 hours and the amount of transported HA* was expressed as a percentage of the total HA* used.

Author Manuscript Author Manuscript Author Manuscript Author Manuscript

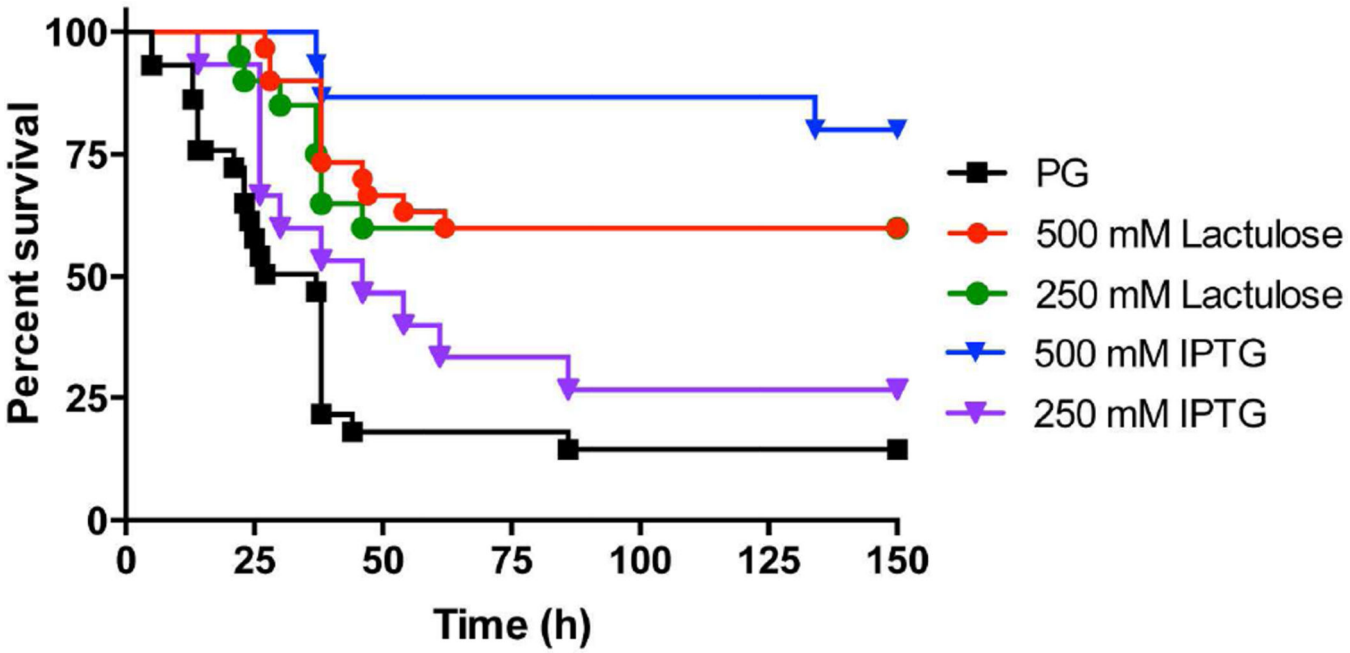

Figure 4. LAU protects mice against BoNT/A oral intoxication

Survival comparisons of mice treated orally with L-PTC/A in the absence (PG: phosphate gelatin) or presence of 250 and 500 mM of LAU and IPTG, respectively. We have reviewed and agreed the policies on Ethics in publishing and Ethical guidelines for journal publication listed on Toxicon website.

Author Manuscript Author Manuscript Author Manuscript Author Manuscript

Table 1

Data collection and refinement statistics

	HA17-HA33-LAU	HA17-HA33-IPTG
Data collection		
Space group	$C222_1$	$C222_1$
Cell dimensions		
a, *b*, c (Å)	107.0, 118.7, 161.8	105.9, 118.9, 162.2
α, β, γ (°)	90, 90, 90	90, 90, 90
Resolution range (Å)	47.8–2.38 (2.51–2.38)[a]	47.95–2.18 (2.30–2.18)[a]
Measured reflections	135,855	177,668
Unique reflections	41,291	53,512
Completeness (%)	99.4 (99.6)[a]	99.6 (93.2)[a]
R_{merge}	4.4 (39)[a]	4.2(41)[a]
$I/\sigma(I)$	14.5 (2.5)[a]	15.1 (2.6)[a]
Structure refinement		
Resolution (Å)	47.8–2.38	47.95–2.18
No. reflections	39,205	50,625
R_{work}/R_{free} (%)	20.3/23.8	22.7/23.8
Restraints (RMS observed)		
Bond length (Å)	0.009	0.008
Bond angle (°)	1.253	1.145
Average isotropic *B*-value ($Å^2$)	63.3	54.0
Number of atoms		
Protein	5,820	5,844
Ligand	46	30
Water	121	171

[a]Values for the highest resolution shells.